Rare Metal Materials and Engineering
Volume 52, Issue 6, June 2023
Available online at www.rmme.ac.cn

Science Press

Cite this article as: Liu Xinglong, Xu Chengyuan, Chen Bin, et al. Influence of Deposition Temperature on Microstructure and Mechanical Properties of TiAlN Coatings for High Performance Manufacture[J]. Rare Metal Materials and Engineering, 2023, 52(06): 2024-2030.

ARTICLE

Influence of Deposition Temperature on Microstructure and Mechanical Properties of TiAlN Coatings for High Performance Manufacture

Liu Xinglong[1,2], Xu Chengyuan[1], Chen Bin[1], Qiao Hong[1], Lin Zeng[1]

[1] School of Mechanical Engineering and Automation, Northeastern University, Shenyang 110004, China; [2] NeuMat (Taian) Surface Technology Limited, Taian 271024, China

Abstract: TiAlN coatings were deposited at various deposition temperatures using vacuum arc ion plating (AIP) for the high performance manufacture. The relationships between deposition temperatures and surface properties were investigated. Results show that surface macroparticles (MPs) decrease in number and size with increasing the deposition temperature because of ion bombardment. When deposition temperature increases, the grain size on the top coating first decreases sharply, and then increases gradually. Furthermore, deposition temperature has little influence on the phase constituents and chemical compositions of the resultant coatings. With raising the deposition temperature, the hardness and adhesion strength first increase rapidly, and then decrease gradually. The deposited TiAlN coating exhibits the highest hardness and the strongest adhesion strength when deposition temperature is set at around 450 °C. The mechanism of the above phenomena is attributed to the variations of microstructure and residual stress between the surface and interface during the deposition process. The resultant coatings have a good thermal stability in air at temperatures up to 900 °C.

Key words: TiAlN coating; deposition temperature; mechanical property; thermal stability; high performance manufacture

TiAlN coatings are widely used as protective coatings in high performance manufacture applications, because of their excellent properties, including high hardness, wear resistance, and superior oxidation resistance[1–3]. Various vacuum deposition processes and facilities have been used to synthesize TiAlN coatings, such as magnetron sputtering[4–5], high-power pulsed magnetron sputtering[6] and arc ion plating (AIP) [7–8]. Among them, AIP techniques are considered to be promising commercial techniques for TiAlN coating deposition, due to high ionization rate, high deposition rate and high kinetic energy[9–11].

Deposition parameters exert considerable influence on the microstructure, mechanical properties, and thermal stability of TiAlN coatings deposited by AIP techniques. Huang et al [12] deposited TiAlN coatings using Ti/Al targets with various concentration ratios by filtered cathodic arc ion plating (FCAIP) system and found that the crystal structure of the TiAlN layer with maximum hardness is a NaCl-B1 structure with the Ti0.5Al0.5 as target. Vereschaka et al[13] prepared a series of Ti-TiN-TiAlN coatings under various nitrogen pressures and investigated the effects of nitrogen pressure on the microstructure and mechanical properties of the resultant coatings. Some researchers[14] studied the effects of bias voltage on the microstructure and properties of TiAlN coatings. However, the influencing mechanism of deposition temperature on the microstructure and properties of TiAlN coatings are still not very clear for the application of high-performance manufacture.

In our previous work, arc cathode equipped with a scanning radial magnetic field was developed and the effect of magnetic field on the microstructure of resultant films was studied [15]. In the present study, an industrial scale setup equipped with an optimized temperature controller was used to prepare hard coatings in order to study the effects of deposition parameters on the surface properties and service

Received date: December 05, 2022
Foundation item: National Natural Science Foundation of China (51775096); Central University Basic Research Fund of China (N2003009); Chinese Academy of Sciences-WEGO Research Development Plan
Corresponding author: Lin Zeng, Ph. D., Professor, School of Mechanical Engineering & Automation, Northeastern University, Shenyang 110004, P. R. China, Tel: 0086-24-8367-6945, E-mail: zlin@mail.neu.edu.cn

performance of the coated samples.

1 Experiment

Mirror-polished M2 high-speed steel plate with the size of 28 mm×18 mm×3 mm was used as the substrate. TiAlN coatings were grown in an industrial-scaled batch-type arc ion plating facility, using powder-metallurgical produced TiAl alloy (Al/Ti atomic ratio was 70∶30, 99.9% purity) as targets (Φ160 mm), as shown in Fig. 1. The surface morphology and cathode spot motion were monitored and then controlled through a steered magnetic field.

At the beginning of coating process, the chamber was evacuated up to a base pressure of less than 8.0×10^{-3} Pa. Meanwhile, the chamber and substrates were heated rapidly and maintained at 420 °C. In the target cleaning for 60 min, high purity Ar gas (99.999% in volume fraction) was introduced into the chamber to a pressure of 4.0×10^{-1} Pa with a flow rate of 150 mL/min. Three Ti (99.9% purity) targets were evaporated by arc-discharge, and the bias voltage applied on the substrate holder was fixed at −150 V. The TiAlN coating was synthesized at 390, 420, 450, and 480 °C, while N_2 partial pressure was kept constantly at 3.8 Pa throughout the coating process. In this experiment, coating deposition time was kept at 3 h. The detailed parameters are listed in Table 1.

The surface morphologies of the samples were observed by field emission scanning electron microscopy (INSPECT F50, Thermo Fisher Scientific, Eindhoven, The Netherlands) equipped with energy dispersive spectroscopy for elemental analysis. The density and diameter distribution of MPs and micro-craters were quantitatively analyzed by image analysis software (ImageJ 1.47). The crystallographic phases of the coatings were examined by X-ray diffractometer (MPDDY2094, PANalytical B. V., Eindhoven, The Netherlands) using a Cu Kα (wavelength λ=0.154 06 nm) radiation source operated at 40 kV and 40 mA. The scanning angle ranged from 30° to 100°, and every sample was scanned for 10 min. The coatings were in situ heated in air from room temperature to 900 °C. The temperature was stabilized every 100 °C for 10 min, and then the XRD data of the coatings was recorded at 700 and 900 °C. The compound structure and level structure were analyzed by X-ray photoelectron spectroscopy (XPS) using Al Kα (hv=1486.6 eV) radiation source (150 W), which was calibrated by carbon peak C 1s at 284.5 eV. Surface roughness was measured with a 3D profilometer.

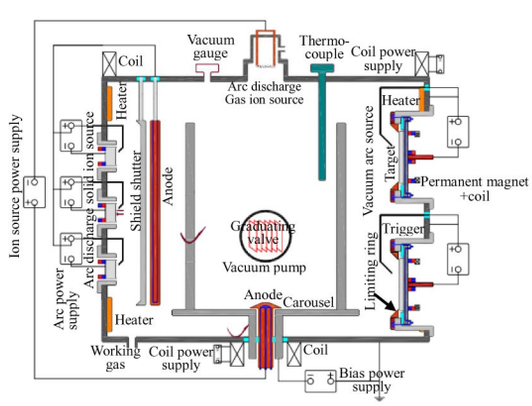

Fig.1 Schematic diagram of industrial-scaled batch-type arc ion plating facility

Table 1 Detailed parameters of AIP process

Parameter	Value
Base pressure/$\times10^{-3}$ Pa	7.0
Working pressure/Pa	3.8
Deposition temperature/°C	390, 420, 450 ,480
Arc current/A	120
Negative bias voltage/V	150
N_2 flow rate/mL·min^{-1}	800–900
Substrate rotation speed/Hz	8
Distance between the target and substrate/mm	100

Adhesion strength was measured with a scratch tester (MFT-4000, Lanzhou Huahui Instrument Technology Co., Ltd, Lanzhou, China) at the loading speed of 100 N/min and maximum scratching length of 10 mm. The critical loads were determined by the acoustic signal. At least four scratch tests were performed on each sample, which was separated by a distance of about 1 mm.

2 Results and Discussion

2.1 Surface morphology

Fig. 2a – 2d present the typical surface morphologies of TiAlN coatings deposited at 390, 420, 450 and 480 °C, respectively. As shown in Fig. 2, the number and size of MPs decrease and micro-craters gradually appear with increasing deposition temperature. Fig. 3 present the density of MPs (d>1 μm) and micro-craters (d>1 μm) on the coated surface synthesized at various deposition temperatures. It can be seen that the density of MPs decreases sharply from 23.3×10^{-3}/μm^2 to 0/μm^2, whereas the density of micro-craters increases rapidly from 1.5×10^{-3}/μm^2 to 7.3×10^{-3}/μm^2 as the deposition temperature increases from 390 °C to 480 °C.

The ion bombardment plays an important role in the elimination of MPs during the AIP process. In our case, the kinetic energy and momentum of incident ions increase with deposition temperature[16]. The higher temperature implies greater local ion and electron pressure gradients, which are the main driving forces for ion acceleration. At the high deposition temperature, the particles have high kinetic energy, and the intense ion bombardment will promote the removal of MPs. At the same time, some micro-craters are left on the

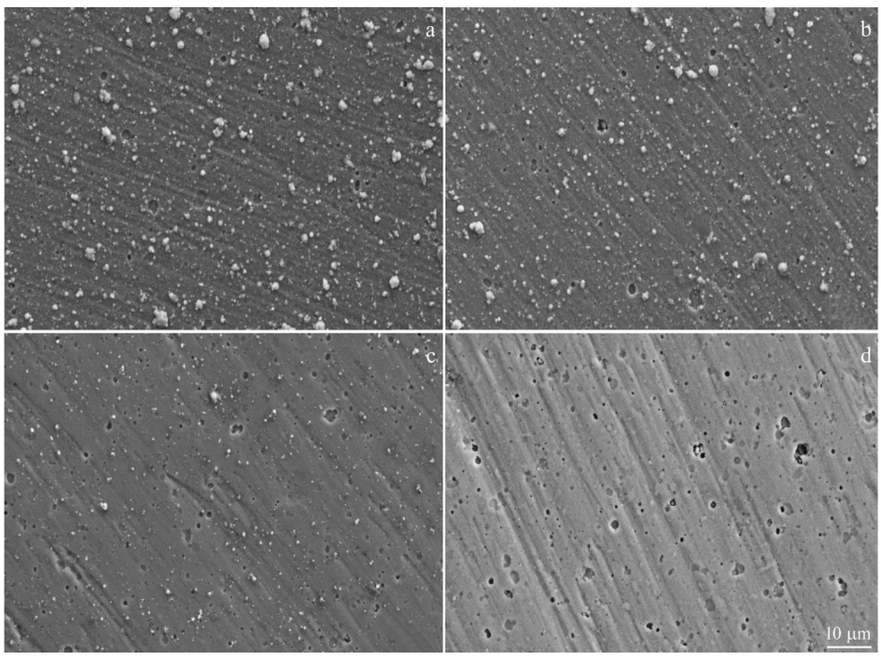

Fig.2 Typical surface morphologies of TiAlN coatings deposited at different temperatures: (a) 390 °C, (b) 420 °C, (c) 450 °C, and (d) 480 °C

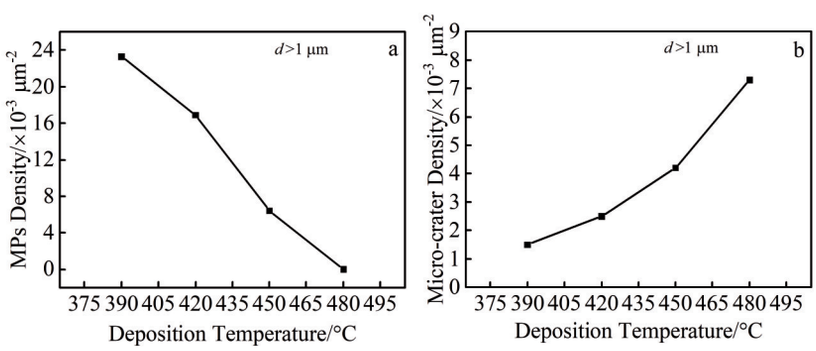

Fig.3 Density of macroparticles (a) and micro-craters (b) in the TiAlN coatings deposited at various temperatures

surface because of the bombardment of incident ions with high energy. The size and depth of micro-craters on the surface both increase with the deposition temperature.

The effects of MPs and micro-craters on the surface roughness were further analyzed. Fig.4 shows the variation of surface roughness S_a as a function of deposition temperature. With increasing the deposition temperature, the surface roughness first decreases sharply and then increases gradually. The minimum value of surface roughness (0.168 μm) was obtained at a deposition temperature of 450 °C. The above variation is in accordance with the relationship between the surface morphology of the coatings and deposition temperature. The effects of deposition temperatures on the surface roughness may be related to the densification phenomena caused by the strong ion bombardment, which will result in reduced MPs and micro-craters.

2.2 Composition and XPS analysis

Fig. 5 presents the chemical compositions of the TiAlN coatings deposited at various deposition temperatures. Accordingly, when the deposition temperatures increase from 390 °C to 480 °C, the Ti, Al, and N contents fluctuate in a small range. The elemental contents increase from 32.28% to 33.7% for Al, and from 18.34% to 19.41% for Ti; the N content decreases from 48.53% to 48.31% correspondingly. These results can be explained by the change of ion energy. The decrease in N content is very complex as the temperature increases. First, nitrogen depletion in the Al-rich domain and a slight enrichment in the Ti-rich domains occur. Next, the Al-rich domains become stoichiometric and the nitrogen deficiency is accommodated in the coarsened Ti-rich domains[17].

The analyses of the surface region of the samples reveal the presence of nitride species on both spectral regions of Ti 2p and Al 2p. After peak fitting for the Ti 2p, Al 2p and N 1s of the TiAlN coatings deposited at various deposition temperatures (Fig.6), the binding energy (BE) positions of the nitrides (on Ti 2p and Al 2p experimental peaks) shift towards low values relative to those predicted by the XPS NIST database and those collected from reported results[18–19].

The Ti 2p spectrum recorded from the coatings is presented in Fig.6a, which reflects two different components. The peaks of Ti 2p at 454.8 and 460.8 eV correspond to the $2p_{3/2}$ and $2p_{1/2}$ levels, respectively. The binding energies of the $2p_{3/2}$ and $2p_{1/2}$

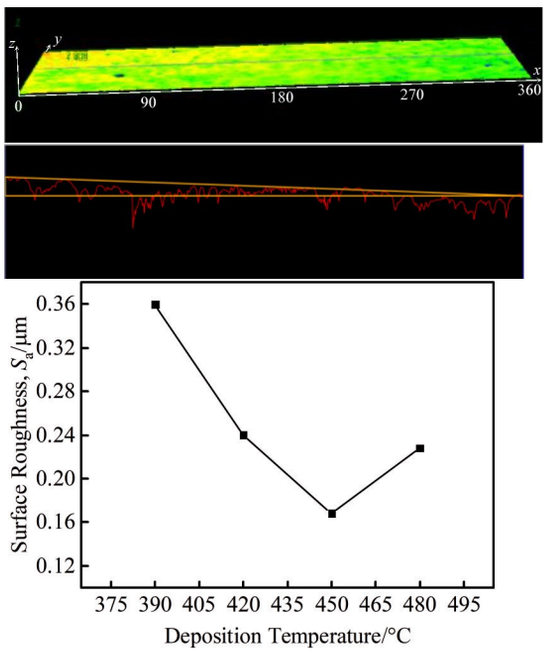

Fig.4 Surface roughness of TiAlN coatings as a function of deposition temperature

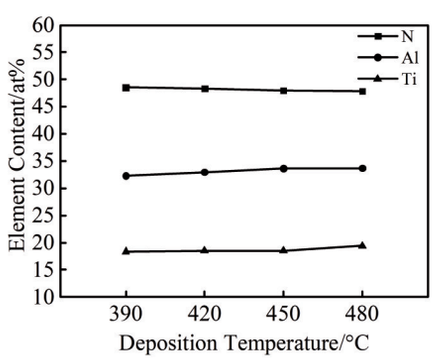

Fig.5 Chemical composition of TiAlN coatings deposited at 390, 420, 450 and 480 °C

levels of this doublet are recognized as TiN and TiAlN, respectively according to Ref.[18–19], thereby indicating the presence of TiN and TiAlN phases. It is found that the peak position of Ti $2p_{3/2}$ moves to a lower angle, which may correlate with the shift to lower angles of the c-TiAlN peaks toward c-TiN. This suggests a nucleation and growth phase transformation mechanism (c-TiAlN/c-TiN+w-AlN) through a continuous depletion of Al from c-TiAlN rather than a formation of c-TiN and c-AlN domains[17]. As shown in Fig. 6b, two different components are revealed after the peak fitting of the Al 2p line: the first one at 73.7 eV is ascribed to AlN, which shifts to 0.2 eV toward a low binding energy with respect to the Al 2p of the TiAlN coating [18–19]; the second one at 74.3 eV is attributed to the TiAlN compound[19]. The N 1s spectrum recorded from the samples is shown in Fig. 6c. The N 1s peaks are decomposed to three peaks at 396.6, 397.2 and 397.4 eV, which stand for AlN, TiAlN, and TiN, respectively[18–19]. According to the results of the XPS, no TiAl phase forms, similar to the other TiAlN reported data[18–19].

2.3 XRD analysis

Fig. 7 shows the XRD patterns of TiAlN coatings deposited at various deposition temperatures. The diffraction peaks of various coatings exhibit similar patterns, which can be identified as the TiN and AlN phases with preferred orientation in the (200) directions at the 2θ values about 41.2° and 43.8°, respectively. (200) preferred orientation of coatings indicates that surface energy and interfacial energy control the preferred orientation, which causes low strain energy. In this case, the crystal structure of coatings is hexagonal wurtzite structure, which leads to grain refinement and thus prevents cracks propagation. The intensities of other diffraction peaks such as TiN (111), TiAlN (200), and TiAlN (311) are considerably low. No signals are related to metal phases in the coatings. The deposition temperatures exert a certain effect on the phase constituents of the coatings, as well as on the positions and intensities of the diffraction peaks. The intensity of diffraction peak of TiN (200) and AlN (200) increases with the deposition temperature, indicating a high degree of crystallinity. At the same time, the position of diffraction peaks of TiN (200) and AlN (200) moves toward a large angle as the deposition temperature increases. The reason is that the change in deposition temperature might have a certain effect on the residual stress of the coatings[20].

On the basis of the quantitative analysis, the average grain size of the AIP TiAlN coatings was calculated by the full-width at half maximum (FWHM) of the strongest AlN (200) diffraction peak in the XRD spectra (Fig. 7) using the Scherrer formula[21–22]:

$$\text{Size} = \frac{0.9\lambda}{B\cos\theta} \quad (1)$$

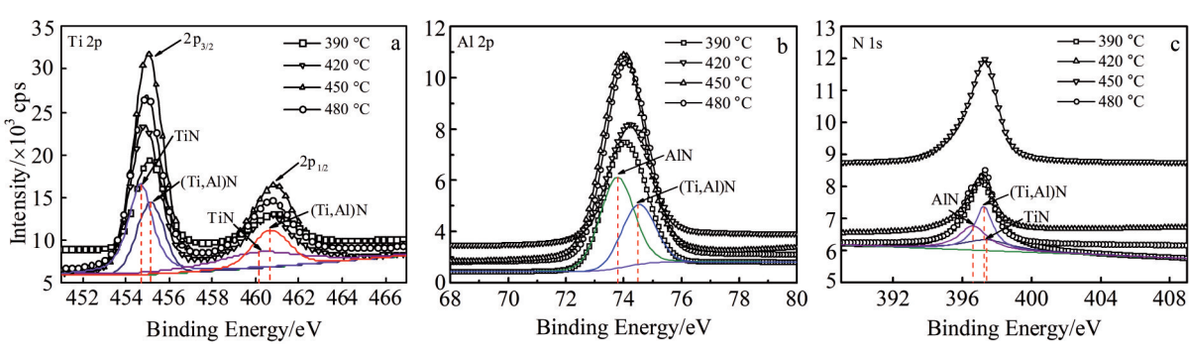

Fig.6 Fitted XPS spectra of Ti 2p (a), Al 2p (b) and N 1s (c) of the coatings deposited at various temperatures

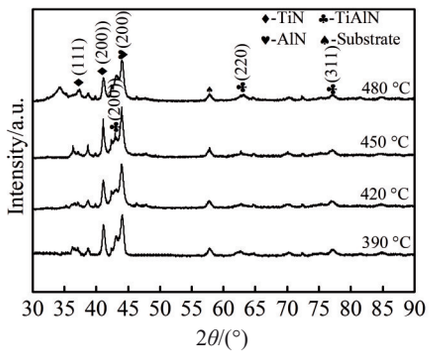

Fig.7 XRD patterns of TiAlN coatings deposited at various deposition temperatures

where λ is the wavelength of Cu Kα radiation, B is the calibrated FWHM of a Bragg peak, and θ is the Bragg angle. The lattice constants of the coatings are also estimated from the interplanar spacing d_{hkl} of the strongest peaks in the XRD spectra using the equation of hexagonal close-packed structure[23]:

$$d_{hkl} = \frac{1}{\sqrt{\frac{4}{3}\frac{h^2 + hk + k^2}{a^2} + \frac{t^2}{c^2}}} \quad (2)$$

where a and c are the lattice constants; h, k, and l are the crystal plane indices.

Fig. 8 presents the calculated results of the average grain size and lattice constant of the AlN phase in the AIP TiAlN coatings at different deposition temperatures. The grain sizes first decrease from 26.1 nm to about 18.4 nm and then increase to about 22.1 nm with deposition temperature. When the deposition temperatures decline to a certain threshold, the incident particles on the sample surface have higher kinetic energy with deposition temperature. Meanwhile, surface mobility increases with deposition temperature[24–25]. Therefore, both ion bombardment and surface mobility work together to make the grain size decrease. In this experiment, TiAlN coatings have a minimum average grain size of approximately 18.4 nm when the deposition temperature is set at 450 °C. However, when the deposition temperatures exceed a certain threshold, film growth mechanism is entirely different. Excessive bombardment of energetic ions at high deposition temperature results in another increase in defect density in the coatings. The variation of grain size with temperature is consistent with that of surface roughness (shown in Fig.4).

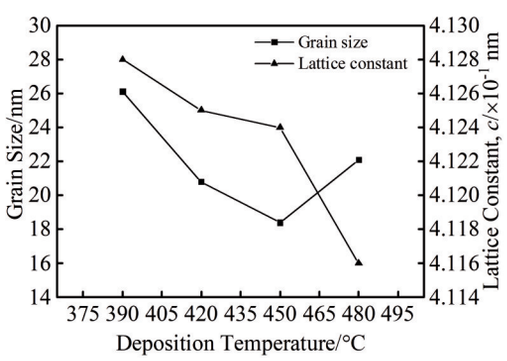

Fig.8 Variations of grain sizes and lattice constants of AlN phase in the TiAlN coatings deposited at different temperatures

Furthermore, as shown in Fig. 8, the lattice constant in the coatings decreases and all lattice constants in the coatings exhibit a negative deviation relative to the standard lattice constant (c=4.978×10^{-1} nm) with increasing deposition temperature. This negative deviation indicates that the compressive residual stresses are introduced in all coatings during the coating deposition process[26–27], and the residual stress increases with deposition temperature. It is believed that the defect density plays an important role in the lattice constants of AlN phase; that is, the low defect density goes against the coating stress release[28].

2.4 Mechanical properties

The hardness values of the TiAlN coatings measured with a microhardness tester are presented in Fig. 9. One thing to be aware of is that the indentation depths need to be less than one tenth of the coating thickness, which are listed in Table 2. All coatings present a high hardness, and the highest coating hardness is obtained when the deposition temperature is 450 °C. With increasing deposition temperature, the hardness of the TiAlN coatings first increases gradually from 23.4 GPa to the maximum value of about 35.6 GPa, and then decreases sharply to 27.6 GPa. The enhanced hardness of the coatings might originate from different hardening mechanisms, which can be divided into two types, namely, intrinsic hardening and extrinsic hardening[29–31].

In the present work, intrinsic hardening exerts a significant effect on the hardness of TiAlN coatings. It is found that the compressive residual stress can significantly improve the coating hardness[26]. The defect density of the coatings also plays an important role in their hardness. Literature indicates that the existence of defects such as micro-craters, MPs in the coatings exert a detrimental effect on the hardness[32–33]. With

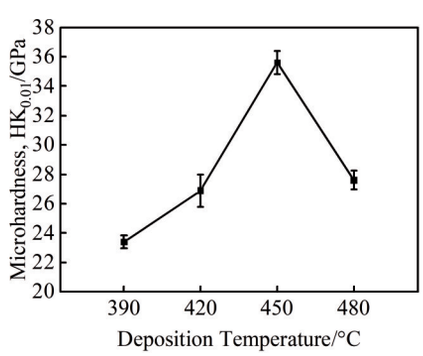

Fig.9 Vickers microhardness of TiAlN coatings deposited at various deposition temperatures

Table 2 Thickness and indentation depth of TiAlN coatings

Deposition temperature/°C	Thickness/μm	Indentation depth/μm
390	2.59	0.23
420	2.81	0.25
450	3.15	0.28
480	3.04	0.26

increasing deposition temperature, the defect density in the coatings changes from more defects to fewer defects, and to more defects again. As a result, the densest microstructure with the least defects and the highest residual stress forms in the coatings at a deposition temperature of 450 °C. Laws of residual stress development are not clear till now, while it is believed that compressive residual stress is dependent on the phase formation and transformation behavior, such as transformation of AlN from cubic to hexagonal.

Changes in the critical load of the AIP TiAlN coatings with deposition temperature are shown in Fig.10. As the deposition temperature increases from 390 °C to 480 °C, the critical load first increases sharply before reaching the maximum value of about 29.7 N and then decreases rapidly. The coating/substrate system has the best adhesion when the deposition temperature is 450 °C. The above trend is in accordance with the relationship between the microstructure of coatings and the deposition temperature, as shown in Fig. 4 and Fig. 8. These phenomena are attributed to the changes in the microstructure of the coatings as the deposition temperature increases, and a few defects in the coatings are helpful in inhibiting the spread and expansion of cracks, which in turn improves adhesion[28]. In addition, the particles have high kinetic energy as the deposition temperature increases. The diffusivity of particles also increases, which can further improve the adhesion of coatings. However, the high deposition temperature indicates higher thermal stress in the coating. A high thermal stress will cause a detrimental effect.

2.5 Thermal stability

The thermal stability of the TiAlN coatings at high temperatures was studied by XRD. Fig. 11 shows the XRD patterns of TiAlN coatings at recording temperatures of 700 and 900 °C. The diffraction peaks of the coatings at 700 °C exhibit similar patterns as the XRD patterns of the coatings at room temperature; no significant phase change takes place. The intensity of the diffraction peak TiAlN (200) increases with the temperature. The coatings contact with the substrate, and no spallation is observed during or after heating. In addition, no signals related to oxide phases are observed in the coatings. Fig. 11b presents the XRD patterns of the TiAlN coatings at 900 °C. With the increase in temperature, the

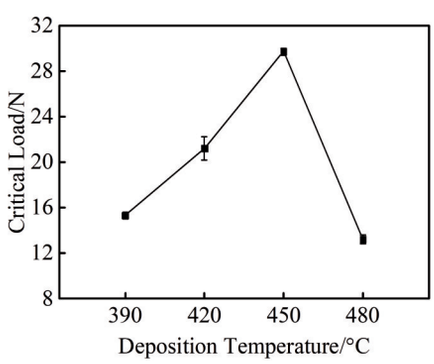

Fig.10 Changes of critical load for TiAlN coatings deposited at various deposition temperatures

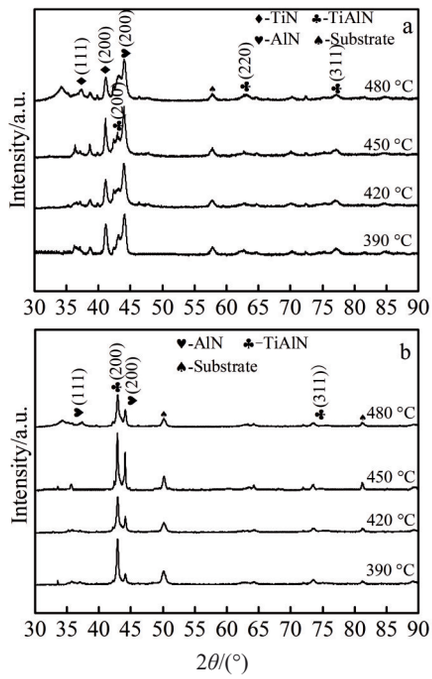

Fig.11 XRD patterns of TiAlN coatings deposited at different temperatures recorded at 700 °C (a) and 900 °C (b)

phase structures changes from the TiN phase and AlN phase to the TiAlN phase. This phenomenon is delayed because of the change in solubility of Al atoms in the solid-solution. However, the intensity of the substrate diffraction peak experiences a certain increase, indicating that the thermal stability of the coatings decreases gradually. The coatings do not exhibit any significant oxidation behavior when the temperature reaches 900 °C. These results indicate that the TiAlN coatings at 900 °C still have good thermal stability.

3 Conclusions

1) The number and size of surface macroparticles decrease, and micro-craters gradually appear with increasing deposition temperature in the TiAlN coatings deposited by vacuum arc ion plating technique. The ion bombardment plays an important role in the elimination of surface macroparticles and the appearance of micro-craters as the deposition temperature increases.

2) The AlN phase and TiN phase with preferred orientations in the (200) directions appear in the resultant coatings. With increasing deposition temperature, the grain size of the TiAlN coatings first decreases slightly, and then increases gradually. However, the lattice constant always decreases gradually with the deposition temperature, which is ascribed to the changes in the defect density of the coatings.

3) Deposition temperature causes the changes in mechanical properties of resultant TiAlN coatings by affecting the microstructure and defect density. With increasing deposition temperature, the hardness and critical load of the TiAlN coatings first increase gradually, then decrease slightly. In this experiment, when the deposition temperature is set at

450 °C, the coatings possess the highest hardness and the strongest adhesion strength.

4) When the service temperature reaches 900 °C, the surface phase structures change from the previous TiN phase and AlN phase to the TiAlN phase. However, the coatings show no significant oxidation behavior, which indicates that the resultant TiAlN coatings possess good thermal stability.

References

1 Zhang Jun, Lv Huimin, Cui Guanying *et al. Thin Solid Films*[J], 2011, 519(15): 4818

2 Xu X, Chen L, Pei F *et al. Surf Coat Technol*[J], 2016, 304: 512

3 An Q L, Wang C Y, Xu J Y *et al. International Journal of Refractory Metals and Hard Materials*[J], 2014, 43: 94

4 Zywitzki O, Klostermann H, Fietzke F *et al. Surf Coat Technol*[J], 2006, 200(22–23): 6522

5 Devia D M, RestrepoParra R, Arango P J *et al. Appl Surf Sci*[J], 2011, 257(14): 6181

6 Greczynski G, Lu J, Johansson M *et al. Vacuum*[J], 2012, 86(8): 1036

7 Xiao B J, Chen Y, Dai W *et al. Surf Coat Technol*[J], 2017, 311: 98

8 Zhao S S, Du H, Zheng J D *et al. Surf Coat Technol*[J], 2008, 202(21): 5170

9 Heidsieck H. *Surf Coat Technol*[J], 1999, 112: 324

10 Wang L, Zhang S H, Chen Z *et al. Appl Surf Sci*[J], 2012, 258(8): 3629

11 Baranov O O, Fang J, Rider A E *et al. IEEE Transactions on Plasma Science*[J], 2013, 41(12): 3640

12 Huang S H, Hsieh T E, Chen J W. *Surf Coat Technol*[J], 2009, 204(6–7): 988

13 Vereschaka A S, Vereschaka A A, Sladkov D V *et al. Journal of Nano Research*[J], 2016, 37: 51

14 Wustefeld C, Rafaja D, Klemm V *et al. Surf Coat Technol*[J], 2010, 205(5): 1345

15 Wang S H, Lin Z, Qiao H *et al. Coatings*[J], 2018, 8(2): 8 020 049

16 Zhirkov I, Oks E, Rosen J. *Journal of Applied Physics*[J], 2015, 117(21): 16

17 Schramm I C, Joesaar M P J, Jensen J *et al. Acta Mater*[J], 2016, 119: 218

18 Greczynski G, Jensen J, Greene J E *et al. Surface Science Spectra*[J], 2014, 21(1): 35

19 Marco J F, Gancedo J R, Auger M A *et al. Surf Interface Anal*[J], 2005, 37(12): 1082

20 Yao Y R, Li J L, Wang Y X *et al. Surf Coat Technol*[J], 2015, 280: 154

21 Bushroa A R, Rahbari R G, Masjuki H H *et al. Vacuum*[J], 2012, 86(8): 1107

22 Klug H P, Alexander L E. *X-ray Diffraction Procedures for Polycrystalline and Amorphous Materials*[M]. New York: Wiley, 1954

23 Jafari M, Vaezzadeh M, Noroozizadeh S. *Metallurgical & Materials Transactions A*[J], 2010, 41(13): 3287

24 Anayara B, Amir H, Atowar R. *Beilstein Journal of Nanotechnology*[J], 2012, 3(3): 438

25 Anders A. *Thin Solid Films*[J], 2010, 518(15): 4087

26 Wang T G, Zhao S S, Hua WG *et al. Mater Sci Eng A*[J], 2010, 527(3): 454

27 Tung H M, Huang J H, Tsai D G *et al. Mater Sci Eng A*[J], 2009, 500(1–2): 104

28 Wang T G, Jeong D, Liu Y M *et al. Surf Coat Technol*[J], 2012, 206(10): 2638

29 Jiang N, Shen Y G, Zhang H J *et al. Mater Sci Eng B*[J], 2006, 135(1): 1

30 Liu Z J, Shum P W, Shen Y G. *Thin Solid Films*[J], 2004, 468(1–2): 161

31 Sakurada E, Hiwatashi S, Ushioda K. *Journal of the Japan Institute of Metals*[J], 2016, 80(10): 655

32 Tung H M, Huang J H, Tsai D G *et al. Mater Sci & Eng A*[J], 2009, 500(1): 104

33 Warcholinski B, Gilewicz A. *Vacuum*[J], 2013, 90(1): 145

沉积温度对高性能TiAlN涂层微观结构和力学性能的影响

刘兴龙[1,2]，徐乘远[1]，陈　彬[1]，乔　宏[1]，蔺　增[1]

(1. 东北大学 机械工程与自动化学院，辽宁 沈阳 110004)

(2. 泰安东大新材表面技术有限公司，山东 泰安 271024)

摘　要：采用真空电弧离子镀（AIP）技术在不同沉积温度下TiAlN涂层，用于高性能制造，并研究了沉积温度与表面性能的关系。结果表明，由于离子轰击作用，表面大颗粒随沉积温度的升高而减少。随着沉积温度的升高，涂层表面的晶粒尺寸先急剧减小后逐渐增大。此外，沉积温度对合成涂层的相组成和化学成分影响不大。随着沉积温度的升高，硬度和粘结强度先迅速增加，后逐渐降低。当沉积温度在450 ℃左右时，沉积的TiAlN涂层硬度最高，粘结强度最大。上述现象的发生机理与沉积过程中表面与界面之间的微观组织和残余应力的变化有关。合成的涂层在高达900 ℃的空气中具有良好的热稳定性。

关键词：TiAlN涂层；沉积温度；力学性能；热稳定性；高性能制造

作者简介：刘兴龙，男，1990年生，博士，东北大学机械工程及自动化学院，辽宁 沈阳 110004，E-mail：425212968@qq.com